



# Application Notes

## ***A Space-Mapped Model of Thick, Tightly Coupled Conductors for Planar Electromagnetic Analysis***

■ James C. Rautio

Accurate modeling of thick metal in a planar electromagnetic analysis can require that the thickness of the metal be divided into a large number of thin sheets or layers, substantially increasing analysis time. This order of modeling is especially important when two thick conductors are separated by less than the metal thickness. This article describes a method to efficiently realize the accuracy of a large number of thin sheets by introducing a “space mapping” layer into a simple model that can be efficiently analyzed.

### **Background**

Thick, closely spaced conductors (Figure 1) represent a major challenge for electromagnetic analysis. To achieve high accuracy, subsection size must be small with respect to wavelength. In addition, the relevant subsection size must be small to accurately represent the current distribution. For thick metal, this means that the subsection thickness must be small with respect to the gap between closely spaced conductors. With a planar analysis, this is achieved by dividing the line thickness into thinner sheets [1] (Figure 2). However, the numerical complexity of the problem increases rapidly with the number of sheets. A similar problem occurs with three-dimensional (3-D) volume meshing electromagnetic (EM) tools where the mesh must be small with respect to the conductor thickness (and small with respect to skin depth when volume currents are used), significantly increasing analysis time.

In order to efficiently analyze thick metal, we modify a two-sheet model so that the results match an extrapolated infinite-

sheet model for a simple structure. Then we use this modified two-sheet model to efficiently and accurately analyze a complicated structure and compare the results with measurement.

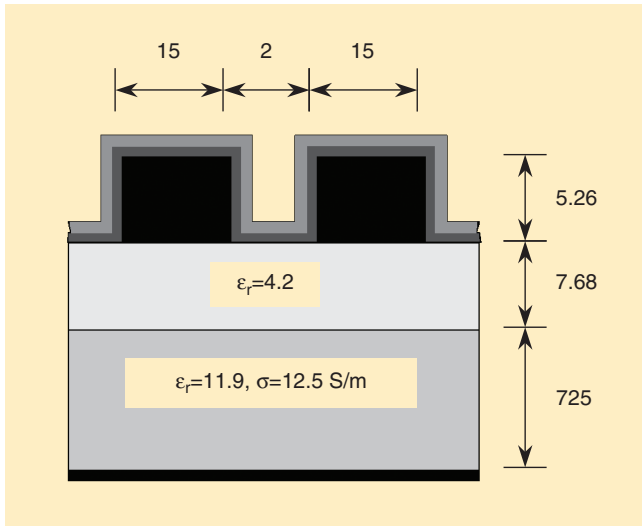
### **Model Development**

The model is developed as follows:

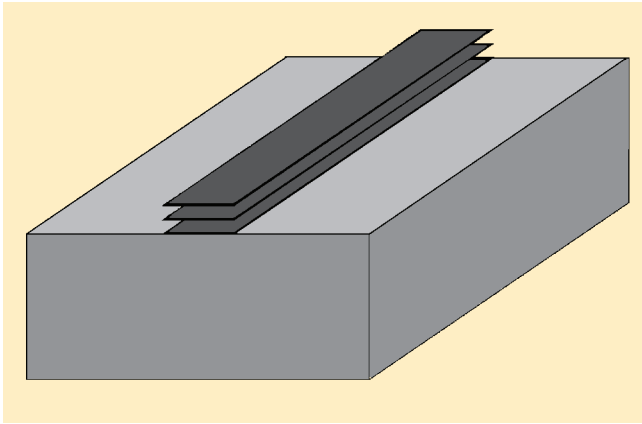
- 1) Analyze a length of coplanar waveguide (CPW) for characteristic impedance and epsilon effective, or equivalently, inductance per unit length and capacitance per unit length. Start with a one-sheet model, and keep increasing the number of sheets until analysis time becomes excessive.
- 2) Use a Richardson extrapolation [2], [3] to evaluate the inductance and capacitance per unit length for an infinite-sheet model of the thick CPW line.
- 3) Modify a two-sheet model of the CPW line by increasing the width of all lines and by inserting a thin “space mapping” layer above the top sheet.
- 4) Modify the permeability and permittivity of the space mapping layer so that the capacitance and inductance per unit length of the two-sheet CPW model match the extrapolated infinite-sheet CPW line.

Figure 3 shows the CPW line cross section selected for Step 1 above. A single dielectric fills the 5.26- $\mu\text{m}$  thick region between the top and bottom surfaces of the thick lines. A composite dielectric constant of 2.7 is selected based on viewing the 2- $\mu\text{m}$  wide volume between the lines (Figures 1 and 4) as a set of series- and parallel-connected parallel plate capacitors. The vertically (i.e., on the sides of the thick transmission lines) deposited layers of passivation dielectric in this region are assumed to be 0.8 times the thickness of the horizontal layers.

James C. Rautio (rautio@sommetsoftware.com) is with Sommet Software, Inc., 100 Elwood Davis Road, North Syracuse, NY 13212 USA +1 315 453 3096.



**Figure 1.** Two thick, closely spaced conductors on silicon. The two thin passivation layers on top of the conductors are detailed in Figure 4. Conductor bulk conductivity is  $3.57 \times 10^7$  S/m. Dimensions are in microns.



**Figure 2.** Cross section of the three-sheet model of a thick transmission line. The longitudinal edges of each sheet are connected together (not shown) to allow current to flow from one sheet to another as needed.

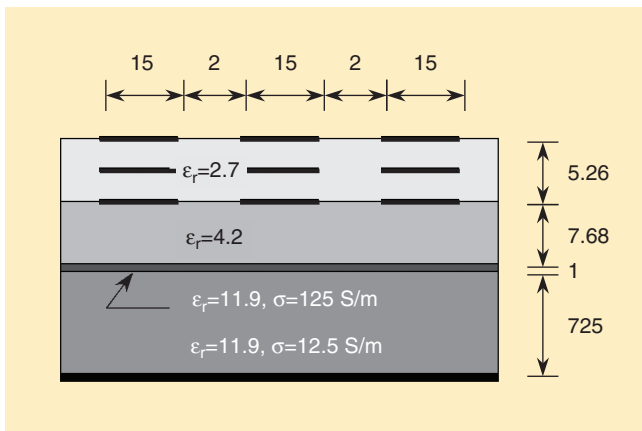


**Figure 3.** Cross section of the CPW line used to develop the thick metal model. The number of sheets (three are shown) is increased to investigate convergence. Dimensions are in microns.

In detail, to calculate the effective permittivity of the gap between two  $5.26\text{-}\mu\text{m}$  thick transmission lines, we calculate the capacitance of three regions (Figure 4) per unit length  $L$ :

1) The capacitance of the very bottom  $0.2\text{-}\mu\text{m}$  thick,  $\epsilon_r = 4.2$  passivation layer is

$$C_1 = \epsilon_0 \times 4.2 \times 0.2 \times L/2.0.$$

2) The capacitance of the  $0.6\text{-}\mu\text{m}$  thick,  $\epsilon_r = 7.0$  passivation layer is the series combination of three capacitances, with  $C_2$  taken twice

$$C_2 = \epsilon_0 \times 4.2 \times 0.6 \times L/0.16,$$

$$C_3 = \epsilon_0 \times 7.0 \times 0.6 \times L/1.68.$$

3) The capacitance of the remaining  $4.46\text{-}\mu\text{m}$  of the gap is the series combination of five capacitances, with  $C_4$  and  $C_5$  each taken twice

$$C_4 = \epsilon_0 \times 4.2 \times 4.46 \times L/0.16,$$

$$C_5 = \epsilon_0 \times 7.0 \times 4.46 \times L/0.48,$$

$$C_6 = \epsilon_0 \times 1.0 \times 4.46 \times L/0.72.$$

4) The capacitance of the entire gap with air substituted for all dielectric is

$$C_0 = \epsilon_0 \times 1.0 \times 5.26 \times L/2.0.$$

5) The effective permittivity of the  $5.26\text{-}\mu\text{m}$  layer is then

$$\epsilon_{\text{eff}} = \left[ C_1 + \frac{1}{\frac{2}{C_2} + \frac{1}{C_3}} + \frac{1}{\frac{2}{C_4} + \frac{2}{C_5} + \frac{1}{C_6}} \right] \frac{1}{C_0}.$$

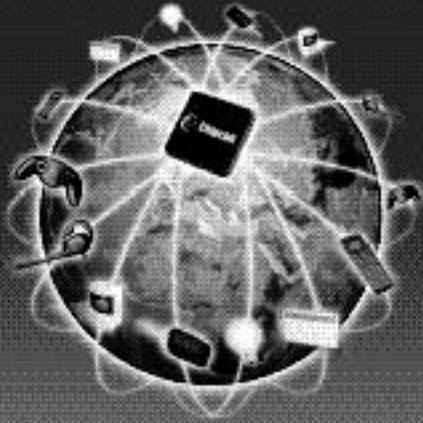
The CPW line is  $256\text{-}\mu\text{m}$  long, the box sidewalls are  $47\text{ }\mu\text{m}$  from the outside edge of each outer ground strip, and a  $2.0 \times 0.5\text{-}\mu\text{m}$  cell size is used. Also included is a  $1\text{-}\mu\text{m}$  thick high conductivity layer, as discussed in the next section.

Table 1 shows the result of increasing  $N$ , the number of sheets in the analysis.  $N$  is one more than the number of contained dielectric layers. The number of dielectric layers is doubled in each case. Since the change in  $L$  and in  $C$  decreases by about half each time the number of dielectric layers ( $N-1$ ) is doubled, we can apply a Richardson extrapolation; the result is in the final row. The analysis times shown in Table 1 are for a 3-GHz P4. Drawing a large number of sheets for analysis is tedious, but this task is now automated [4], including automated inclusion of vias connecting all longitudinal edges.

For the second step of the above algorithm, a two-sheet model is selected and a “space mapping layer” is introduced. Space mapping maps a “fine” model that has high accuracy to a “coarse” model that has low accuracy but can be analyzed quickly [5]. In this case, the infinite-sheet model is the fine model and the two-sheet model of Figure 5 is the coarse model.

As typically applied, space mapping determines the correlation between the fine and coarse models. Then, the coarse model is quickly analyzed and optimized with the results translated back to the fine model. Here, we physically modify the coarse model so that it provides the same results as the fine model. Thus, the space mapping is performed internally to the model. This is known as “implicit space mapping” [6], [7].

When there is no space mapping layer, the two-sheet model ( $N = 2$  in Table 1) shows less capacitance and more inductance per unit length than the extrapolated infinite-sheet model ( $N = \infty$  in Table 1). We make two modifications



# Market Leading Short Range RF-ICs

300-1000 MHz and 2.4 GHz single-chips.  
Narrowband, Multi-channel and Spread Spectrum

Wireless applications in:

- Home and Building Automation
- Automatic Meter Reading
- Alarm and Security Systems
- Consumer Electronics
- Automotive

Leading provider of IEEE 802.15.4 and ZigBee™ technology

Chipcon AS, Gaustadalleve 77, NO-2007 Oslo, Norway  
Tel: +47 22 55 86 44 Fax: +47 22 55 89 96  
E-mail: sales@chipcon.com  
www.chipcon.com

to the two-sheet model in order to realize the same CPW inductance and capacitance as the extrapolated infinite-sheet model. Depending on the specific situation, the designer may wish to use only one or the other of these modifications.

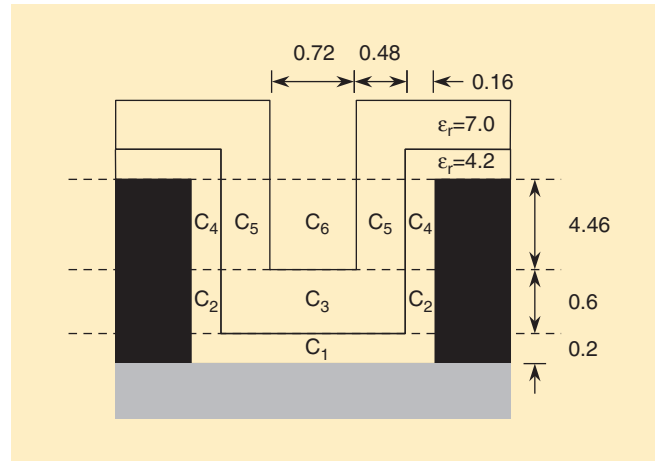


**Figure 4.** Cross-sectional detail of the gap area and passivation dielectric. The gap is modeled based on an effective permittivity determined by calculation of the indicated capacitances between the sides of the metal lines (black). Dimensions are in microns.

**Table 1. Convergence of N-sheet model.**

N	L (nH/m)	C (pF/m)	Analysis Time (s)
1	296	133	4
2	188	165	17
3	168	184	39
5	154	201	144
9	146	211	346
17	143	216	2,131
∞	140	221	N/A

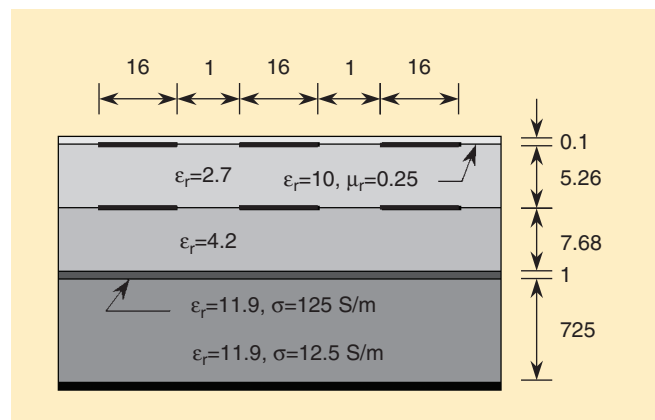


**Figure 5.** The permittivity and permeability of a “space-mapping” layer (on top) is set so that the resulting capacitance and inductance per unit length is the same as the extrapolated infinite-sheet model. Dimensions are in microns.

For the first modification, we increase the width of all lines, in this case, by  $1\ \mu\text{m}$ . The increased width decreases the CPW inductance. Increasing the line width also decreases the gap width. The decreased gap width increases the CPW capacitance. However these modifications do not completely relieve the CPW capacitive deficit and inductive excess.

For the second modification, we add a thin space mapping layer. This is the top dielectric layer in Figure 5. The thickness is arbitrarily selected by the designer, but it should be kept thin compared to line thickness. The space-mapping layer permittivity and permeability are adjusted so that analysis of the space-mapped model yields the same capacitance and inductance as the infinite-sheet model. This is done by trial

and error. The required repeated EM analyses proceed quickly because the inductance depends only on the space-mapping layer permeability, and the capacitance depends only on the permittivity. Even so, automated optimization of this task would be useful. The capacitance and inductance of a transmission line can be calculated from the characteristic impedance and epsilon effective or by specifying automatic generation of transmission line parameters in the EM analysis.

### Applying the Model

To check the space-mapped model, the gap width is swept from 2 to  $12\ \mu\text{m}$  in steps of  $2\ \mu\text{m}$ . In all cases, the space-mapped thickness model yields an epsilon effective no more than 0.1% different from the 17-sheet model and a characteristic impedance no more than 2% different for large gaps. Using the same space mapping layer for a  $10\text{-}\mu\text{m}$  wide line yields about the same differences over the same 2- to  $12\text{-}\mu\text{m}$  gap range. This model is applicable to both regular (rectangular) meshing and to conformal meshing [8], allowing efficient analysis of thick circular spiral inductors, as well as rectangular spirals.

Several configurations of the space-mapping model were considered. Of these, the configuration of Figure 5 provides the best agreement as gap and line width are swept. One other option considered was to space map a one-sheet model, however, the required inductance and capacitance changes are larger, and agreement as width and gap are swept is not as good. Such a model may be appropriate if numerical requirements of a two-sheet space-mapped model are excessive.

We apply the space-mapped model of Figure 5 to a five-turn spiral inductor. A  $1.0\text{-}\mu\text{m}$  cell size is used, and analysis time is 15 min, 34 s per frequency on a 3-GHz Pentium. Analysis at six frequencies is required to provide interpolation to the full, spectrally rich, result from 0.1 to 20 GHz. If desired, faster analysis can be easily achieved by using only the space-mapping layer (no change in line width) combined with coarser (but less accurate) meshing. As described below, much faster analysis time is realized if the CPW ground cage is removed.

Figure 6 shows measured versus calculated data. The intended application requires results valid to 10 GHz. Above 10 GHz, it was found that including the vias, which connect the CPW ground strips (at the indicated reference planes) to the substrate ground plane, is important. The

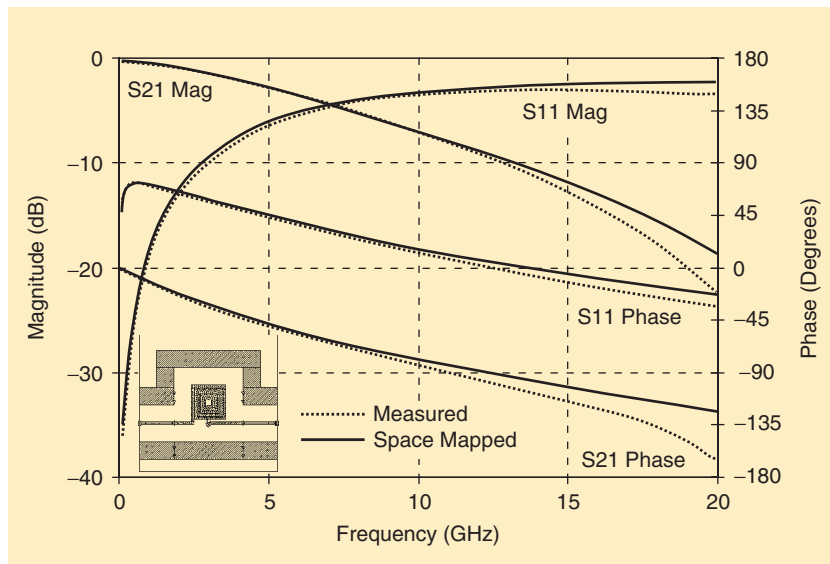


**Figure 6.** Measured versus space-mapped two-sheet thick metal model for the five-turn spiral inductor. The one-sheet model is used for the CPW ground strips.

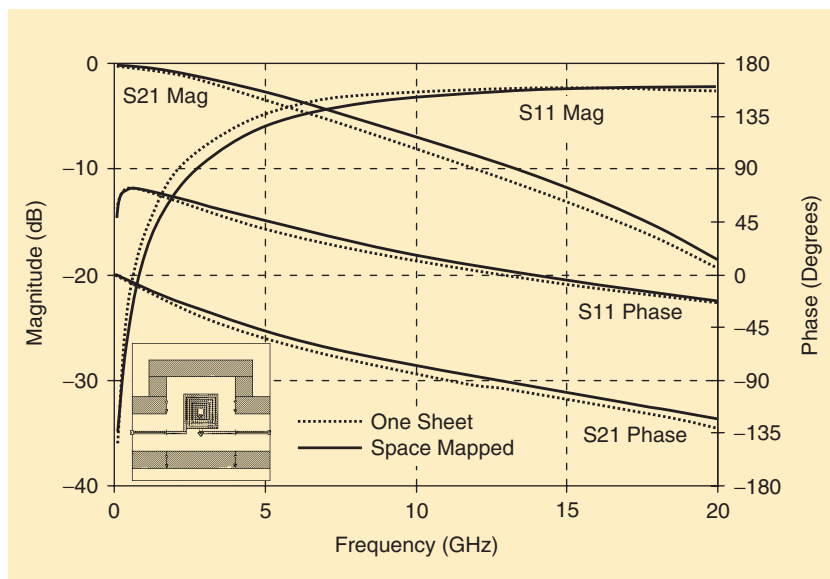


**Figure 7.** The one-sheet conductor model shows differences from the space mapped two-sheet thick metal model that render it unusable for the intended application. This figure effectively shows the effect of thickness on the inductor.

**First the  
FPD1000AS  
and FPD2000AS,  
and now...**

**the FPD4000AF,  
from...**

The Semiconductor  
Operation at  
Filtronic Semilab is now  
Filtronic Compound Semiconductors

### Filtronic Compound Semiconductors

Filtronic Compound Semiconductors, Inc. announces the addition of the FPD4000AF to its new line of Power pHEMT products including the FPD1000AS and FPD2000AS. The FPD4000AF is a high power, flange mount packaged device, ideally suited for power applications in L-Band. The FPD4000AF is a 4 watt (typical 36.5dBm) device featuring excellent linearity and efficiency at frequencies through 4GHz. Typical applications include drivers or output stages in PCS/Cellular base station transmitter amplifiers, as well as other power applications in WLL/WLAN amplifiers.

The FPD1000AS and FPD2000AS are surface mount devices ideally suited for applications requiring high gain, efficiency, and linearity. Typical uses include output stages for picocell transmitters, drivers for higher power base station requirements, or Fixed Wireless Access applications through 3.5GHz. The FPD1000AS is a 1 watt (typical 31 dBm) device featuring 16 dB linear gain at 1.8 GHz when tuned for best linearity. The FPD2000AS offers 2 watts with 15dB linear gain. Both devices offer excellent linearity, as you would expect from pHEMT technology. Performance is characterized at a supply of 10 volts.

These are the first offerings in a family of devices which is planned to include higher power levels at frequencies through 3.5 GHz, as well as C-band and Ku-band power FETs.

Samples of the FPD4000AF, FPD1000AS and FPD2000AS are available from stock. Specifications can be found at [www.filcs.com](http://www.filcs.com). For further information...



**Filtronic Compound Semiconductors**

Visit our website at [www.filcs.com](http://www.filcs.com)

10181 Burbank Road, Cupertino, CA 95014-4133  
Phone (408) 850-5790 • FAX (408) 850-5766  
Contact: [sales@filcs.com](mailto:sales@filcs.com)

calculated current distribution shows that above 10 GHz ground return current starts to flow preferentially through the substrate and substrate ground, rather than through the CPW ground strips.

The 1- $\mu\text{m}$  thick layer (Figures 4 and 5) was not included in initial analyses of this inductor, and the difference between measured and calculated was of concern. Convergence analysis with respect to cell size, number of sheets, and sensitivity analysis with respect to physical geometry indicated that numerical uncertainty and fabrication uncertainty could not explain the observed difference. Numerical experiments then showed that an additional thin, high-conductivity layer could explain much of the difference. Upon careful investigation it was then found that a high-conductivity layer (a 1- $\mu\text{m}$  thick CMOS PWELL layer) did indeed exist. Performing a high-confidence convergence and sensitivity analysis was critical in making this discovery.

Significant difference (with respect to the uncertainty suggested by convergence and sensitivity analyses) still exists above 10 GHz. This difference could be caused by a difference between the structure that was analyzed and that which was measured. We are not currently aware of any such physical differences that could cause the observed difference in results. Other possible causes for the difference include an additional currently unidentified loss mechanism or measurement error.

The calculated inductor self-resonant frequency (inductance = 0) is higher than measured. The space mapping layer has almost no effect on the self-resonant frequency, suggesting that the interturn capacitance does not play the expected role in establishing the self-resonant frequency.

Although it might not be critical in this case, the ground strips should be symmetrical so as to keep the CPW ground return current balanced on each side. For full accuracy, the calculated results should be modified for the effect of unbalanced CPW ground return current on the measurement equipment [10]. This was not done here and may possibly explain the difference in resonant frequency. To eliminate this potential source of error, the CPW ground cage, when used, should always be perfectly symmetrical for each ground strip.

We emphasize very strongly that if a component is measured with a CPW ground cage, and then it is used or analyzed without a ground cage, one should expect different results to be obtained.

### Effect of Thick Metal

The data of Figure 6 uses the simple one-sheet model for the thick CPW ground strips. The inductor was also analyzed using the space-mapped two-sheet thick metal model for the CPW ground. There is no discernable difference in the results when plotted. The one-sheet model is adequate and should be used for any conductors that are not tightly coupled to other conductors.

Figure 7 shows the space-mapped thick-metal model compared to the entire inductor analyzed using the one-sheet model. This figure can be viewed as the effect of thickness on this inductor. These differences are unacceptable for the intended application (general purpose high frequency design).

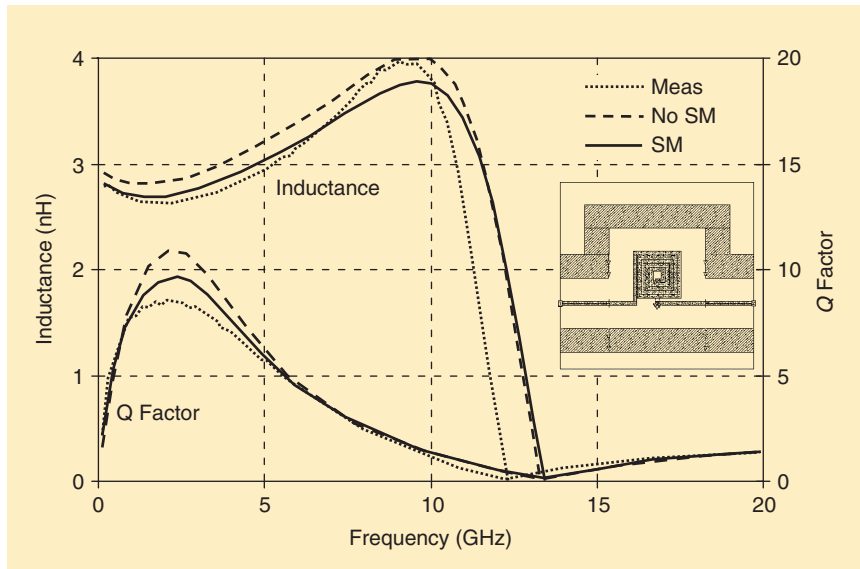


**Figure 8.** Measured (dotted line) inductance and Q factor for the five turn spiral compared with the space mapped (solid line, SM) result and with the same inductor analyzed without space mapping (dashed line, No SM).

When the two-sheet model of the inductor is analyzed with the original  $15\text{-}\mu$  wide lines and no space-mapping layer, S-parameters change by up to 1 dB, with larger changes at higher frequencies. Calculated inductance (Figure 8) increases by about 5% over the entire band below resonance. Calculated maximum Q increases by 14%, the frequency of maximum Q remains unchanged. The space-mapped calculated Q is 11% higher than the measured Q. This is similar to other thick-metal-small-gap spirals that have been analyzed using this approach. The calculated Q can be made to match the measured Q almost exactly if the conductivity of the metal is reduced; however, even though the required reduction is small, it is inconsistent with measured dc conductivity.

With confidence in the space-mapped, thick-metal model, one may now conduct numerical experiments to determine the effect of CPW ground strip layout ("cage design"). In particular, the effect of ground strip removal, which forces microstrip operation, can be determined. For this design, operating in the microstrip mode was found to be significantly different from the CPW mode only above 10 GHz.

Without the CPW ground strips, analysis time drops to 5 min per frequency and only five frequencies are required for interpolation. To correctly analyze the microstrip mode response, one must make sure the side walls that parallel the port connecting transmission lines are far from the inductor so that ground return current is forced to flow through the substrate and substrate ground and not through the side walls. Accurate analysis also requires several other important considerations. Primary among these is that the geometry

that is analyzed be as close as is reasonably possible to what is measured. For example, the Jazz inductor was fabricated and measured with a CPW ground cage. The ground strips also use vias to connect to the substrate ground. Both are important in the overall response at high frequency.

## Conclusion

A space-mapped two-sheet model for thick metal has been introduced. The model modifies a "coarse," less accurate, but fast two-sheet model so that it provides the same result as a "fine," accurate but slow extrapolated infinite-sheet model. This thick-metal model is appropriate for tightly coupled lines, especially when the gap is less than the metal thickness. The model is validated for a five-turn spiral inductor on silicon.

## Acknowledgment

Densely populated inductors are difficult to accurately model because of the large ac resistance caused by current crowding [9], prompting this research. The data and technology information on this inductor, which was used to verify the space-mapped model, was provided by Volker Blaschke from Jazz Semiconductor.

## References

- [1] J.C. Rautio and V. Demir, "Microstrip conductor loss models for electromagnetic analysis," *IEEE Trans. Microwave Theory Tech.*, vol. 51, pp. 915–921, Mar. 2003.
- [2] R.C. Booton, *Computational Methods for Electromagnetics and Microwaves*. New York: Wiley, 1992.
- [3] W.H. Press, B.P. Flannery, S.A. Teukolsky, and W.T. Vetterling, *Numerical Recipes*. Cambridge, U.K.: Cambridge Univ. Press, 1986.
- [4] Sonnet version 9.0, Sonnet Software, North Syracuse, NY.
- [5] J.W. Bandler, R.M. Biernacki, S.H. Chen, P.A. Grobelny, and R.H. Hemmers, "Space mapping technique for electromagnetic optimization," *IEEE Trans. Microwave Theory Tech.*, vol. 42, pp. 2536–2544, Dec. 1994.
- [6] J.W. Bandler, M.A. Ismail, and J.E. Rayas-Sánchez, "Expanded space mapping EM-based design framework exploiting preassigned parameters," *IEEE Trans. Circuits Syst. I*, vol. 49, pp. 1833–1838, Dec. 2002.
- [7] J.W. Bandler, Q.S. Cheng, N. Georgieva, and M.A. Ismail, "Implicit space mapping EM-based modeling and design using preassigned parameters," *IEEE MTT-S IMS Digest*, Seattle, WA, 2002, pp. 713–716.
- [8] J.C. Rautio, "A Conformal Mesh For Efficient Planar Electromagnetic Analysis," *IEEE Trans. Microwave Theory Tech.*, vol. 52, pp. 257–264, Jan. 2004.
- [9] W.B. Kuhn and N.M. Ibrahim, "Analysis of current crowding effects in multiturn spiral inductors," *IEEE Trans. Microwave Theory Tech.*, vol. 49, pp. 31–38, Jan. 2001.
- [10] T. Jamneala, P.D. Bradley, and D.A. Feld, "Employing a ground model to accurately characterize electronic devices measured with GSG probes," *IEEE Trans. Microwave Theory Tech.*, vol. 52, pp. 640–645, Feb. 2004. 